





## Article

# An Intensity-Variation RI Sensor for Multi-Variant Alcohol Detection with Twisted Structure Using Polymer Optical Fiber

Abdul Ghaffar <sup>1,†</sup>, Rehan Mehdi <sup>2,†</sup>, Irfan Mehdi <sup>2</sup>, Bhagwan Das <sup>3</sup>, Vicky Kumar <sup>4</sup>, Sadam Hussain <sup>1,\*</sup>, Gul Sher <sup>2</sup>, Kamran Ali Memon <sup>5</sup>, Sikandar Ali <sup>6</sup>, Mujahid Mehdi <sup>7,\*</sup> and Khurram Karim Qureshi <sup>5</sup>

- <sup>1</sup> Key Laboratory of Air-Driven Equipment Technology of Zhejiang Province, College of Mechanical Engineering, Quzhou University, Quzhou 324000, China; 92ghaffar@gmail.com
- <sup>2</sup> Dr. M. A. Kazi Institute of Chemistry, University of Sindh, Jamshoro 76080, Pakistan; rehanmehdi000@gmail.com (R.M.); irfanmehdi512@gmail.com (I.M.); gulsherkhaskheli10@gmail.com (G.S.)
- <sup>3</sup> Design and Creative Technology Vertical, Torrens University, Ultimo, NSW 2007, Australia; bhagwan.das@torrens.edu.au
- <sup>4</sup> Civil and Environmental Engineering, Universiti Teknologi Petronas, Seri Iskandar 32610, Malaysia; vicky.kumar@utp.edu.my
- <sup>5</sup> IRC-CSS, King Fahd University of Petroleum & Minerals, KSA, Dhahran 31261, Saudi Arabia; ali.kamran77@kfupm.edu.sa (K.A.M.); kqureshi@kfupm.edu.sa (K.K.Q.)
- <sup>6</sup> University of Chinese Academy of Sciences, Beijing 101408, China; alisikandar26@mails.ucas.ac.cn
- <sup>7</sup> Faculty of Design, Aror University of Art Architecture Design & Heritage Sindh, Sukkur 65200, Pakistan
- \* Correspondence: sadamhussain@qzc.edu.cn (S.H.); mmehdi.faculty@aror.edu.pk (M.M.); Tel.: +86-155-3690-3568 (S.H.); Fax: +86-570-8015112 (S.H.)
- † These authors contributed equally to this work.

**Abstract:** This research introduces an RI sensor for detecting various alcohol species with a designed twisted polymer optical fiber (POF) sensor. The sensor is developed via a straightforward twisting technique to form an effective coupling mechanism. The sensor works on intensity variation where coupled intensity varies when different types of alcohol are added. The structure relies on the twisting of two fibers, where one fiber is used as the illuminating fiber and the other fiber is used as the receiving fiber. Five different types of alcohol are tested (methanol, ethanol, propanol, butanol, and pentanol) as a substance. The experimental results reveal that the sensor is able to detect all five distinct substances effectively by optical power intensity variation. Moreover, the sensor's sensitivity is analyzed with different factors such as the influence of the bending radius and the coupling length, which reveals that the sensing parameters could be customized depending on specific requirements. The sensor demonstrated consistent responses in repeatability tests, with minimal variation across multiple measurements, highlighting its stability. Additionally, the study explores temperature's influence, revealing a sensitivity shift for every degree Celsius of change. This POF-based alcohol sensor represents a significant leap forward in optical sensing technology.

**Keywords:** POF-based sensor; alcohol sensor; coupling method; intensity-based sensor



**Citation:** Ghaffar, A.; Mehdi, R.; Mehdi, I.; Das, B.; Kumar, V.; Hussain, S.; Sher, G.; Memon, K.A.; Ali, S.; Mehdi, M.; et al. An Intensity-Variation RI Sensor for Multi-Variant Alcohol Detection with Twisted Structure Using Polymer Optical Fiber. *Chemosensors* **2024**, *12*, 252. <https://doi.org/10.3390/chemosensors12120252>

Received: 15 October 2024

Revised: 26 November 2024

Accepted: 1 December 2024

Published: 3 December 2024



**Copyright:** © 2024 by the authors. Licensee MDPI, Basel, Switzerland. This article is an open access article distributed under the terms and conditions of the Creative Commons Attribution (CC BY) license (<https://creativecommons.org/licenses/by/4.0/>).

## 1. Introduction

The need for a precise, rapid, and trustworthy method to detect alcohol levels is crucial across various domains such as the food-processing industry, clinical settings, medical research, and environmental and agricultural evaluations [1–3]. Consequently, continuous monitoring of atmospheric alcohol content is vital for safeguarding workplace health [4–7]. Numerous methods for detecting alcohol have been utilized to examine different substances within complex samples. These techniques include chromatography, immunochromatography, mass spectrometry, nuclear magnetic resonance, polymerase chain reaction, ultraviolet–visible spectroscopy, Fourier-transform infrared spectroscopy (FTIR), standard infrared spectroscopy, surface-enhanced Raman spectroscopy (SERS),

Raman spectroscopy, circular dichroism spectroscopy, spectrofluorimetry, and more, all of which remain highly pertinent [8–18].

Despite their usefulness, these methods have constraints, with some suffering from insufficient precision and accuracy issues. Issues related to ease of movement, delayed reaction times, and complex operational steps emphasize the necessity for fresh analytical strategies that offer swift targeted assessments and clear understanding of outcomes. Exploring the creation of optical fiber sensors as an alternative to established techniques is a potential solution to overcome these difficulties [19,20]. One of the key benefits of optical sensors is their heightened sensitivity and selectivity, enabling exact detection and measurement. These sensors operate in a non-intrusive manner, preserving the original state of the sample and preventing any contamination. They also stand out due to their robust resistance to electromagnetic interference, guaranteeing precise functionality even in adverse conditions. With their long-lasting durability and minimal maintenance needs, optical sensors have solidified their reputation as a dependable option across various sectors [21]. These advantages showcase optical fiber's significant potential for application in both chemical and biological sensing fields.

Optical sensing techniques have long been recognized for their effectiveness in alcohol detection. Fiber optic near-infrared spectroscopy was introduced as a tool for measuring alcohol levels about three decades ago [22]. Since then, significant advancements have been made to enhance sensitivity. A remarkable innovation was the integration of fiber optics with multi-walled carbon nanotubes and  $\text{Co}_3\text{O}_4$ , which achieved heightened sensitivity—35 counts per ppm for ethanol and 51 counts per ppm for ammonia—while also offering exceptional discriminatory capabilities in gaseous substance analysis [23]. Another sensor in alcohol detection technology includes a surface plasmon resonance (SPR)-enabled glass rod sensor design, where the sensor excelled in selectively sensing water and ethanol [24]. Another optical configuration involved an alcohol sensor constructed with lipophilic Reichardt's dyes embedded in polymer membranes, but its functionality is constrained by the influence of pH variations in the solution [25]. Penza et al. combined single-walled carbon nanotubes with silica optical fiber and a quartz crystal microbalance to create a novel alcohol sensor design [26]. Furthermore, an optical microfiber sensor was employed for the detection of alcohol [27]. However, the number of researchers has detected alcohol based on the refractive index change to modulate the optical power intensity.

These sensors work based on the principle that alcohol presence or concentration can change how light travels through a material. Specifically, alcohol alters the material's refractive index. By measuring this change in the refractive index, the sensors can accurately determine the level of alcohol present [28–30]. Morisawa et al. [28] reported a polymer optical fiber-based alcohol sensor in their work, wherein changes in the refractive index were induced by Nonolac resin, which swells upon exposure to alcohol. The SPR optical fiber sensor system is also used for alcohol detection, with an integrated gold layer developed. Notably, this design omitted the need for a rotating stage or spectrometer. Its efficacy in precisely quantifying various alcohol types was then successfully demonstrated through validation tests [29]. A demonstration showcased a tapered fiber optic sensor proficient in identifying aliphatic alcohols, including methanol, ethanol, 1-propanol, and 2-propanol [30]. The sensor operates by detecting alterations in the refractive index within the evanescent field of the fiber's tapered zone, induced by the presence of these alcohols, which in turn modifies the output power. These illustrations demonstrate the advancement in and potential of optical sensing systems in alcohol detection, although with several challenges to overcome.

This research utilizes a POF RI sensor to detect various types of alcohol. The sensor design uses the fiber-twisting technique to obtain intensity variation as the different types of alcohol used for detection purposes. Extensive experimental results were conducted to evaluate the sensor's response and evaluate the sensor's sensitivity performance. This paper's second section discusses the sensor's design and fabrication process, as well as its

underlying operational principles and the specifics of the experimental setup. Results and discussions are subsequently presented in the third section.

## 2. Fabrication and Operation Principle

### 2.1. Sensor Fabrication

This research employs a commercial POF (1 mm step-index SK-40) manufactured by Mitsubishi Co., Ltd. In the SK-40 step-index fiber, the RI experiences an abrupt shift at the interface of the core and cladding layers. Here, the fiber core portion is responsible for light transmission and is made up of polymethyl methacrylate (PMMA), a prevalent transparent polymer material, and the cladding is made of a fluorinated polymer exhibiting a reduced refractive index. This difference ensures the occurrence of total internal reflection of the light rays. Specifically, the POF has a core diameter of 98  $\mu\text{m}$ , paired with a refractive index of 1.49. The core is an encircled 20  $\mu\text{m}$ -thick cladding layer with a refractive index of 1.41, which establishes the vital optical disparity crucial for efficacious light guidance.

For the sensing probe, two POF fibers are used to create twisting structures, as a single fiber is not able to detect alcohol. The twisting creates a coupling structure where the coupled power is affected by a coupling medium. Creating a twist in two POFs involves intertwining them to form a helical structure, similar to how one might twist together two strands of rope or wire. This process can be beneficial for several reasons in optical fiber applications. The twisting structure keeps the fibers closely bound, preventing gaps from forming between them. In contrast, a parallel fiber structure carries the risk of separation between the fibers. When a twisted pair of fibers is bent or pulled, the twist helps distribute the mechanical forces evenly between the fibers, reducing the likelihood of damage. In certain specialized applications, intentionally twisting fibers can enhance the coupling efficiency of light between fibers.

The process of creating a twist in POFs typically involves manually rotating one fiber around the other while maintaining tension control to ensure even twisting and prevent over-twisting. The number and tightness of the twist (number of twists per unit length) can be adjusted based on the specific application requirements. We kept 1 cm for one twist. In the case of the third configuration (extended length), there were 5 twists and the length was 50 mm. After twisting, the fibers can be secured in position using a sheathing material to maintain the twisted configuration. The light source was coupled to the first fiber, and the intensity was measured from the forward end of the fiber. A visual representation of the completed work is provided in Figure 1. A laser diode operating at 635 nanometers (TLS001-635 Thorlabs) was connected with the illuminating fiber and a pair of photodiodes (S120 Thorlabs) was connected with the forward end of the fibers. In previous research efforts [31–34], the concept of a twisted structure has been employed by various scientists for diverse applications.

### 2.2. Sensor Principle

The twisting structure depends on three sensing mechanisms. In a few cases, the twisted structure was used for a rotational sensor [31,32], where the sensing mechanism relies on the coupling of macrobend loss. The continuous bending of the fiber to induce light leakage is a means of detecting movement or rotational motion. In another work [34], a force sensor was developed specifically to work on the principle of cladding mode frustrating total internal reflection. This refers to a situation where the total internal reflection of light within the fiber is disturbed by the introduction of a perturbation in term of force, allowing some light to escape. Contrasting with these prior works, our present study introduces a different operational principle. Instead of relying on macrobend loss or cladding mode disruptions, we employ a change in the refractive index as the fundamental mechanism driving our sensor's function. This approach offers unique advantages and sensing capabilities tailored to the detection and measurement of variations in the refractive properties of the medium surrounding or interacting with the optical fiber.

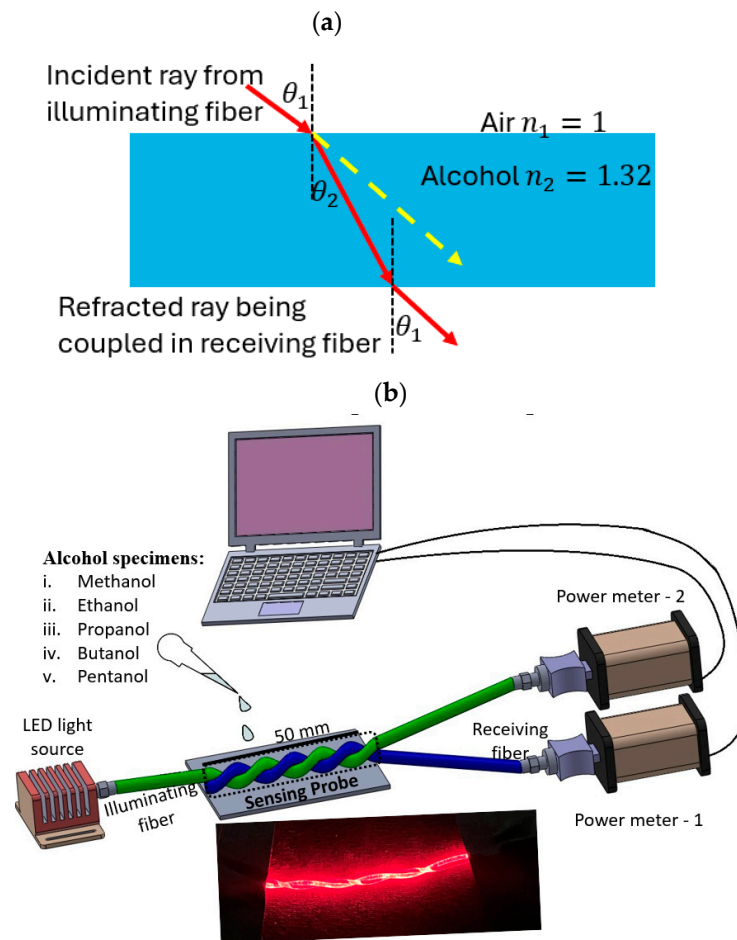


**Figure 1.** (a) Sensing mechanism and (b) illustration of sensor fabrication and experimental setup.

**Boundary Conditions:** In coupled mode theory, solving the differential equations for governing power transfer between fibers requires appropriate boundary conditions specific to the sensor's configuration. For our twisted POF sensor, the boundary conditions are established based on the physical setup of the fibers and the light propagation behavior:

**Input Condition:** At the start of the illuminated fiber ( $z = 0$ ), the power in the illuminating fiber ( $P_1$ ) is equal to the input power from the light source. This is defined as  $P_1(z = 0) = P_{input}$ , where  $P_{input}$  is the optical power injected into the illuminated fiber.

**Coupled Power Condition:** At the receiving fiber's output ( $z = L$  where  $L$  is the length of the twisted region), the coupled power ( $P_2$ ) is measured. This is influenced by the coupling coefficient  $\kappa$  and the refractive index of the surrounding medium. The conditions are:

$$P_2(z = L) = \kappa P_1(z = L) \quad (1)$$

In our experiments, the coupling coefficient is directly influenced by the refractive index of the surrounding alcohol medium. For instance, higher refractive indices (e.g., butanol, pentanol) result in increased  $\kappa$ , leading to higher power transfer. Lower refractive indices (e.g., ethanol, water) exhibit reduced  $\kappa$ , leading to lower coupled power. Moreover, the boundary conditions for the twist length ( $L$ ) and fiber geometry (diameters of the illuminating and receiving fibers) are varied experimentally to optimize coupling efficiency.

**Coupled Mode Theory Derivation:** When a POF undergoes twisting, its functionality evolves into that of an efficient coupling mechanism. In coupled mode theory, the coupling between two optical fibers is affected by several factors, including changes in the surrounding refractive index. In our case, each alcohol sample has a unique RI. When the refractive index of the medium surrounding the fibers changes, it can alter the coupling efficiency between the fibers by impacting the propagation constant and the overlap of the

evanescent fields. This relationship can be described using coupled mode equations. For two coupled fibers, the power transfer between them can be expressed as [35]:

$$\frac{dP_1}{dz} = -\kappa P_2 \ \& \ \frac{dP_2}{dz} = -\kappa P_1 \quad (2)$$

where  $P_1$  and  $P_2$  are the optical powers in fibers 1 and 2, respectively,  $z$  is the propagation direction, and  $\kappa$  (kappa) is for the coupling coefficient between the fibers. The coupling coefficient  $\kappa$  depends on the overlap of the mode fields and the surrounding refractive index.

*Coupling Coefficient Dependency on Refractive Index:* For a refractive index  $n$ , the coupling coefficient  $\kappa$  can be approximated as:

$$\kappa \propto e^{-\alpha \frac{n_{fiber} - n_{medium}}{n_{fiber}}} \quad (3)$$

where  $n_{fiber}$  is the refractive index of the fiber core;  $n_{medium}$  is the refractive index of the surrounding medium, which is alcohol's RI; and  $\alpha$  is a constant that depends on the fiber geometry and other parameters.

As the refractive index of the surrounding medium  $n_{medium}$  approaches that of the fiber core  $n_{fiber}$ , the coupling coefficient  $\kappa$  increases, allowing more power to transfer between the fibers. Conversely, if the surrounding refractive index is significantly different from the core's refractive index, the evanescent fields are less effective in overlapping, reducing the coupling efficiency.

*Evanescent Field Penetration Depth and Its Role:* The evanescent field associated with cladding modes penetrates the external medium adjacent to the fiber. The penetration depth  $d_p$  of this evanescent field is a measure of how far into the external medium this field extends before its intensity drops to a negligible level. This depth is crucial for understanding and designing sensors. The penetration depth  $d_p$  can be mathematically expressed as [36]:

$$d_p = \frac{\lambda}{2\pi \sqrt{n_{clad}^2 \sin^2 \theta - n_{ext}^2}} \quad (4)$$

where  $\lambda$  is the wavelength of the light in a vacuum,  $n_{clad}$  is the refractive index of the cladding,  $n_{ext}$  is the refractive index of the external medium, and  $\theta$  is the incident angle. Thus, a change in the refractive index of the surrounding medium directly affects the amount of power coupled between the fibers. This principle is particularly used in our sensing applications, where changes in the surrounding refractive index can modulate coupling efficiency, enabling the detection of different alcohols.

### 2.3. Characterization of Alcohol Species

The research encompassed investigations on five distinct alcohol species: methanol, ethanol, propanol, butanol, and pentanol. These diverse alcohol specimens were acquired from Sinopharm Chemical Reagent Co., Ltd., Shanghai, China. The refractive indices of pure alcohol forms were determined utilizing an Abbe refractometer, with all readings taken at ambient temperature (20 °C). The refractive indices of various alcohols are important for understanding their optical properties. The RIs of methanol (methyl alcohol), ethanol (ethyl alcohol), propanol (propyl alcohol), butanol (butyl alcohol), and pentanol (amyl alcohol) are approximately 1.329, 1.361, 1.377, 1.397, and 1.410, respectively as shown in Table 1. To conduct the tests, a precise quantity of the alcohol sample was extracted from the flask using a dropper and applied to the twisted structure's sensing probe. Light propagated from one fiber to another fiber is disrupted with a specific RI medium, as shown in Figure 1b. These observed modifications are fundamentally linked to changes in the refractive index and alcohol-specific absorption traits.

**Table 1.** The RI of alcohol species.

No	Species	RI
1	Methanol (methyl alcohol)	1.329
2	Ethanol (ethyl alcohol)	1.361
3	Propanol (propyl alcohol)	1.377
4	Butanol (butyl alcohol)	1.397
5	Pentanol (amyl alcohol)	1.410

### 3. Results and Discussion

Fiber irregularities, including cuts or adjustments similar to those employed in sophisticated technologies such as SPR sensors or D-shaped sensors, can impact the sensor’s output [37,38]. Nonetheless, these methods are typically associated with high expenses or fiber damage. In response to non-destructive and cost-effective sensing techniques, the fiber-twisting approach is an alternative option. This approach entails establishing a deliberate coupling zone within the fiber, designed to facilitate enhanced light interaction with the ambient medium, such as water or alcohol, thereby optimizing sensing capabilities. Figure 2 shows the primary sensor detection response to alcohol, where a straight fiber was also tested. Figure 2 displays the intensity (mW) at the forward end of the illumination fiber over time (sec) under different conditions: without coupling, and with coupling in air and alcohol. The coupled power, denoted as normalized optical power ( $P_2/P_1$ ), was calculated using the outputs, where  $P_2$  represents the final output power and  $P_1$  the initial output power from the same port. The sensor’s sensitivity was defined as:

$$S = (\Delta \text{normalized optical power} / \Delta n) \times \% \tag{5}$$

where  $\Delta n$  denotes the change in the RI of the tested alcohol, and  $\Delta \text{normalized optical power}$  represents the alteration in the coupling ratio. There is no response to the presence of alcohol (see the red curve of Figure 2a). The red line shows a constant intensity over time, indicating that when the fiber is straight and connected to a light source and power meter without any imperfections or coupling, it is not sensitive to the alcohol application in this setup. The sensor response to detecting alcohol is shown in black in Figure 2. The blue and black lines show variations in coupled power when alcohol is applied to the fiber sensor section. The blue line indicates the response when air is replaced with alcohol in the coupling region, showing a noticeable drop in intensity, which demonstrates the sensor’s sensitivity to alcohol.

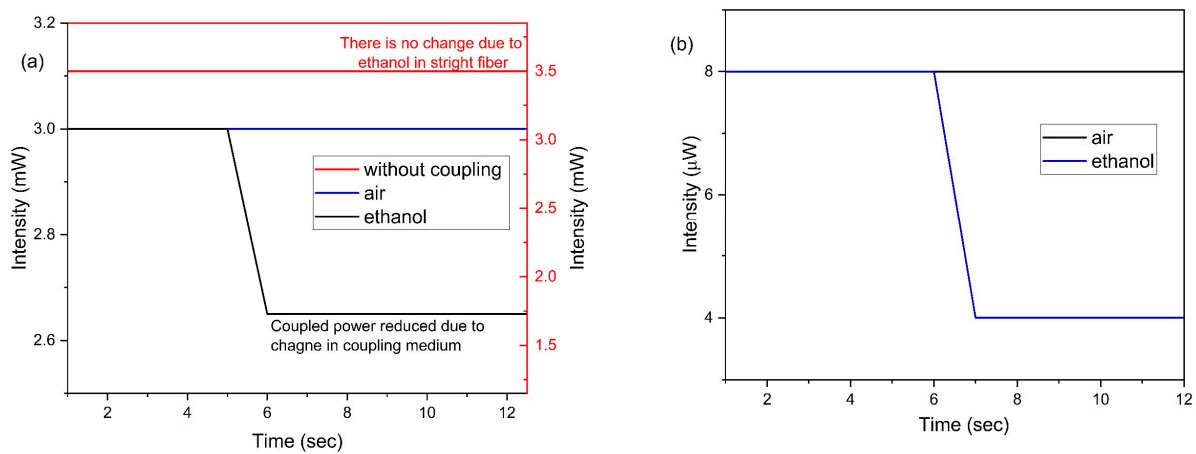


**Figure 2.** Intensity response of the sensor at the end of both fibers over time: (a) illuminating fiber and (b) receiving fiber.

Investigation of the spectral characteristics of the twisted structure was conducted and the experimental setup featured a broadband light source (Ocean Optics DH-2000) that spanned wavelengths ranging from 215 to 2000 nanometers, alongside a spectrometer (Ideaoptics NOVA) for spectral analysis. This setup facilitated exact measurements of the optical responses of the fiber system to various media. The experimental protocol involved illumination connected with a broadband light source, and each forward end was connected with a spectrometer. The resultant data are presented in Figure 3. In Figure 3, the vertical axis labeled “Photon Counts” represents the number of photons detected by the photodetector during the measurement process. Photon counts are directly proportional to the intensity of light that is transmitted through the POF and subsequently detected in the receiving fiber. It reflects the decrease in photon counts as light interacts with the alcohol medium surrounding the fiber. In the twisted structure, the transmitting and coupling ends exhibit a significant increase in coupled loss compared to an untwisted fiber when alcohol is added. The coupling power is further reduced in the receiving fiber when alcohol is added.

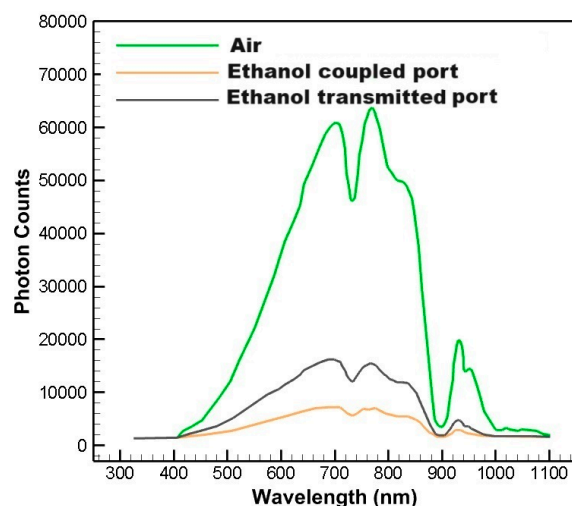
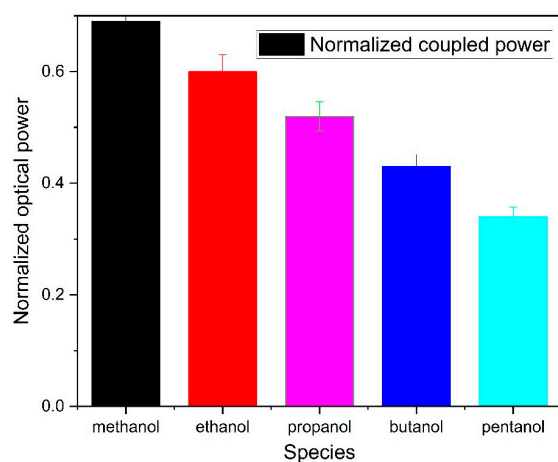


**Figure 3.** Response of the transmission spectra in the transmitted port and in the coupled port.

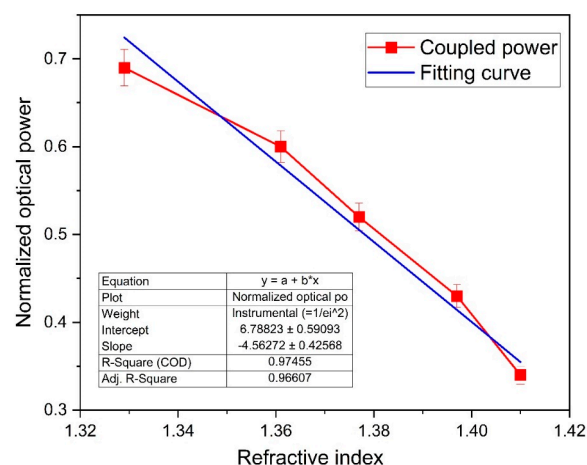
The operational effectiveness of this sensor in distinguishing between different types of alcohol is visually demonstrated in Figure 4. The twisting of the fiber structure introduces a considerable improvement in sensing technology. By intentionally introducing twists, a specialized region is created within the fiber where light can couple or interact more dynamically with the substance outside the fiber, such as alcohol. This coupling region functions as a sensing probe, enabling the fiber to perceive alterations in the external environment. When alcohol is added to the coupling region, it causes a significant decrease in the coupled intensity. This decline in light intensity is in response to the presence of alcohol. Consequently, this methodology offers an economically prudent and fiber-preserving strategy for harnessing optical fibers in sensing applications. Further, a series of different detailed assessments and characterizations were executed to analyze the sensor’s performance and credibility. These assessments are aimed at analyzing the sensor’s sensitivity response, which could be useful for customizing the parameters depending on specific requirements.

Figure 5 illustrates the alcohol-sensing capabilities of the sensor, which is configured with an illuminated fiber and a receiving fiber. Figure 5 highlights the sensor’s ability to differentiate between various alcohols based on their refractive indices and the corresponding changes in power output. With the twisted section measuring precisely 8 mm, the graph discloses a clear linear correlation between the coupling ratio, expressed as normalized optical power, and the RI of the external medium. Notably, as the RI ascends beyond 1.329, coinciding with the POF’s cladding RI, there is a decline in normalized optical power. On the flip side, in cases where the RI dips beneath 1.410, as observed with pentanol, an increase in normalized optical power is evident. This observed trend stems

from the conversion of cladding modes into radiation modes, a phenomenon triggered when the RI of the surrounding alcohol matches the cladding RI, thereby lessening the coupling efficiency. Thus, the sensor excels in detecting RIs that exceed the inherent RI of the fiber cladding. Moreover, the sensor manifests a linear response within the RI spectrum spanning from 1.329 to 1.410.



**Figure 4.** Measured output power of the twisted sensor under various alcohols.



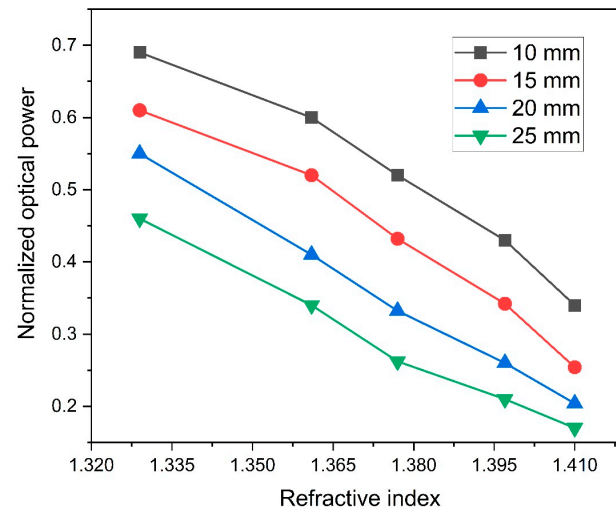
**Figure 5.** Demonstrated alcohol-sensing capabilities configured with an illuminated fiber and a receiving fiber.

Figure 6 illustrates the results of alcohol-sensing experiments conducted on a series of sensors, all featuring an illuminating fiber with a different bend radius. These sensors incorporated bending with four different radii: 10 mm, 15 mm, 20 mm, and 25 mm. When an optical fiber is bending, some of the guided light is radiated out of the core, leading to bending loss. The amount of light that is lost depends on the radius of the bend; smaller bend radii cause greater bend loss due to the tighter curvature. In a twisted optical fiber sensor, the bending induces more significant radiation loss. Meanwhile more radiated power will be coupled. The light-coupling intensity has a direct impact on the bend radii. Thus, for a smaller bend radius, the optical power loss increases more rapidly as the refractive index of the surrounding medium changes. This is because the evanescent field, which extends into the surrounding medium, is more strongly affected by the refractive index changes in a tightly bent fiber.

As the refractive index increases, more light is coupled out of the core, leading to a larger change in the detected optical power. Therefore, sensors with smaller bend radii (10 mm and 15 mm) exhibit higher sensitivity to refractive index changes, as even slight variations in the surrounding medium's refractive index cause significant changes in the



optical power. In contrast, sensors with larger bend radii (20 mm and 25 mm) experience less bend loss and weaker mode coupling. The evanescent field interaction with the surrounding medium is less pronounced, resulting in smaller changes in optical power for the same refractive index variations. As a result, these sensors show reduced sensitivity to refractive index changes because the optical power remains relatively stable, even as the surrounding medium's refractive index changes. Overall, the sensitivity response of the sensors is shown in Table 2.



**Figure 6.** Effect of different bend radii on sensor measurement response.

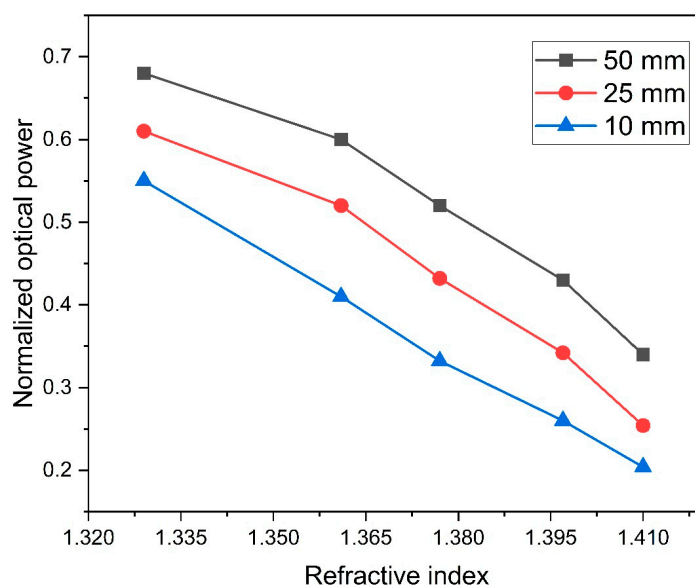
**Table 2.** Sensitivity response of the sensors.

No	Species	R <sup>2</sup>	Sensing Length	Bend Radius
Without bend	178%/RIU	0.9745	10 mm	-
With bend	416%/RIU	0.9821	-	10~50 mm
Extended length	572%/RIU	0.9891	10~50 mm	-

It was observed that the sensor's sensitivity improves when the smaller bend radius is based on the experimental outcomes, whereas the reverse scenario leads to reduced sensitivity. Because a small bend radius generates a higher radiation mode. Meanwhile, it is worth noting that the sensing length also effects the sensor's performance [32,33]. In the context of optical fiber sensors, the influence of the twisted region's length on sensing performance was also investigated, as shown in Figure 7. With increased twisted region length, the interaction between the light in the core and the surrounding medium (i.e., the alcohol solution) is enhanced, as the twisting causes the light to repeatedly interact with the cladding and the external environment. This results in more significant changes in the optical power in response to variations in the RI of the surrounding medium.

A longer twisted region means that the cumulative effect of the twisting perturbations on the light propagation is greater. Each twist contributes to the modulation of the light path, increasing the sensitivity of the sensor to changes in the external refractive index. As the length of the twisted region increases from 10 mm to 50 mm, the overall effect of the twisting is more pronounced, leading to higher sensitivity. This is because the longer twisted region allows for more substantial light interaction with the surrounding medium, amplifying the sensor's response to refractive index changes. The twisted region effectively increases the interaction length between the guided light and the surrounding medium. A longer interaction length means that even small changes in the refractive index can cause more significant alterations in the light propagation, resulting in higher sensitivity. The sensitivity of the alcohol-sensing performance increases with the length of the twisted region due to enhanced mode coupling, accumulated effects of twisting, and increased

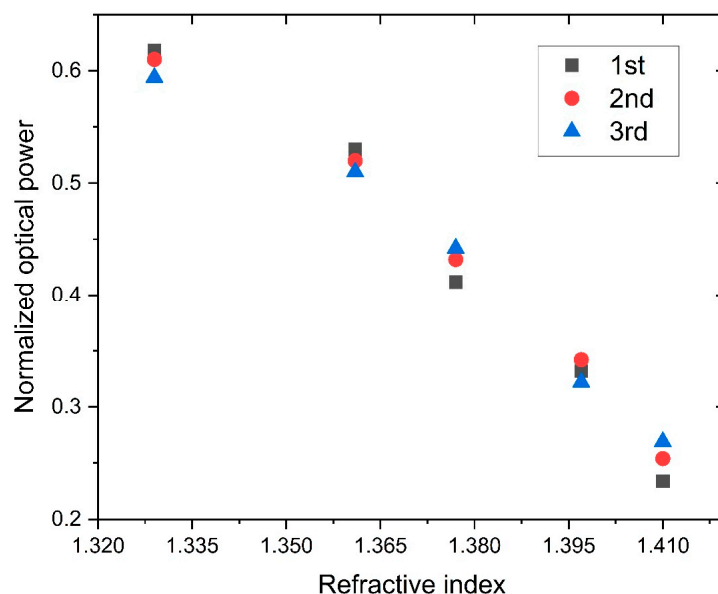
interaction length. These factors collectively amplify the sensor's response to changes in the surrounding medium's refractive index, leading to higher sensitivity with longer twisted regions.



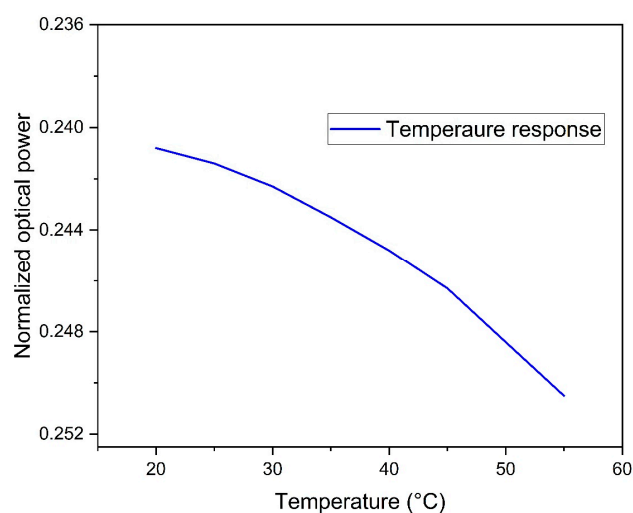
**Figure 7.** Influence of the twisted region's length on the alcohol sensor's performance.

Figure 8 demonstrates the sensor's repeatability by illustrating that the sensor consistently responds when the same alcohol is tested multiple times. The error bars in this figure represent the variability observed across repeated trials, which underscores the reliability and consistency of the sensor's performance. The normalized optical power is plotted against the refractive index of the alcohol samples for three successive measurements, denoted as the first, second, and third time. The data points for the first (squares), second (circles), and third (triangles) measurements show consistent trends across the different refractive indices. This indicates good repeatability of the sensor, as the results from the three measurements are closely aligned. The overlap of data points from the three measurements for each refractive index value demonstrates the sensor's ability to produce reproducible results. There is minimal deviation between the measurements, which signifies the sensor's reliability in repeated use. As the refractive index increases from 1.329 to 1.410, the normalized optical power decreases, following a consistent pattern across all three measurements. This consistent decrease highlights the sensor's sensitivity and stable performance in detecting changes in refractive index.

Figure 9 illustrates the effect of the temperature on the sensor's sensing capability. For the temperature response, the twisted region was placed on a heating plate, and we slowly changed the temperature from 20 °C to 55 °C. We found that for every 5 °C the temperature changes, the sensor's response changes a little. This small change happens because of two main reasons: the thermo-optic effect and heat, which makes the fiber grow or shrink a bit (thermal expansion). When it is warmer, the fiber's ability to bend light changes, which can change light propagated inside the fiber. Also, as the fiber heats up or cools down, it gets bigger or smaller, causing tiny changes in its shape. Temperature changes also cause physical expansion or contraction of the fiber material due to thermal expansion. In the case of twisted structure, this can lead to minute adjustments in the fiber's geometry, such as its diameter, the tightness of the twist (pitch), or the spacing between fibers. These geometric alterations can disrupt the way light is guided and coupled within the fiber, thereby influencing the sensor's output and contributing to its temperature sensitivity.



**Figure 8.** Repeatability sensor response.



**Figure 9.** Influence of temperature on the sensor's performance.

A comparison of fiber optic-based alcohol sensors is shown in Table 3. Its non-intrusive design supports repeated use, and its simplicity in manufacturing promises affordability. It also has a negligible response to temperature fluctuations, flexible fiber configurations, and a mostly straightforward reaction pattern, so integrating this sensor into monitoring equipment is effortless. It is also chemically resilient, compatible with a wide array of solvents, and can be adjusted to suit specific needs, making it a formidable asset for meticulous alcohol detection in applications like chemical analyses, quality checks, and healthcare diagnostics. The sensor's working principle is based on intensity modulation, and concentration and different kinds of isomers are not considered in this study. The sensor's structure will be modified to investigate isomers or concentrations of alcohol. Further studies could involve the incorporation of surface modifications or coatings specifically tailored to interact with certain chemical groups present in alcohol but absent in other volatile organic compounds (VOCs). By introducing these modifications, the sensor can interact with alcohols through additional mechanisms such as hydrogen bonding, hydrophobic interactions, or specific binding, rather than just relying on changes in the refractive index. This approach can significantly enhance the specificity of the sensor, allowing it to distinguish between alcohol and other VOCs more effectively.

**Table 3.** A comparison of fiber optic-based alcohol sensors.

Ref.	Method	Variant	Sensitivity	Fiber
[7]	Finite-element-method	Methanol, ethanol, and propanol,	92%	Photonic crystal fiber
[22]	Spectroscopy	Ethanol	-	Silica fiber
[24]	SPR	Ethanol	-	Silica fiber
[28]	Refractive index	Ethanol, methanol	-	POF
[39]	COMSOL	Ethyl alcohol	44.85%	PCF
[40]	Evanescent field	Alcohol	3.87 dB/%	SMS
[41]	fluorescence intensity	Methanol, ethanol, and propanol	5–90% <i>v/v</i>	-
[42]	Piezoresistive	Ethanol		Poly acrylamide hydrogels
This work	Intensity variation	Methanol ethanol, propanol, butanol, pentanol	572%/RIU	POF

#### 4. Conclusions

This research introduces an RI sensor for detecting various alcohol species using a twisted polymer optical fiber sensor. The sensor is developed via a straightforward twisting and bending principle. The sensor operates on intensity modulation, which changes due to different alcohols altering the coupling medium. The system consists of two fibers: The first fiber launches the light, and the second fiber measures the coupled intensity. The experimental results reveal that the sensor is capable of detecting all five distinct substances. Moreover, the sensor's sensitivity is analyzed with respect to various factors, such as the influence of the sensor bending radius and sensor length. The sensor demonstrates high stability and repeatability, achieving a sensitivity of about 572%/RIU. Additionally, this study explores the influence of temperature, revealing a sensitivity shift for every degree Celsius of change. This POF-based alcohol sensor represents a significant leap forward in optical sensing technology. In future, the sensor's capability to detect additional alcohol types and other volatile organic compounds will be investigated to broaden its applicability in various industries. Long-term stability and durability tests will be conducted to assess the sensor's performance over extended periods and in harsh conditions, improving its robustness for industrial applications.

**Author Contributions:** Conceptualization, S.H.; Data curation, S.A.; Formal analysis, I.M., G.S. and M.M.; Methodology, A.G., V.K. and S.A.; Validation, R.M., K.K.Q. and K.A.M.; Writing—original draft, A.G.; Writing—review & editing, B.D., K.A.M., K.K.Q. and M.M. All authors have read and agreed to the published version of the manuscript.

**Funding:** This research was supported by Zhejiang Provincial Natural Science Foundation of China under Grant No. TGN23E050001.

**Institutional Review Board Statement:** Not applicable.

**Informed Consent Statement:** Not applicable.

**Data Availability Statement:** The data presented in this study are available on reasonable request from the corresponding authors.

**Conflicts of Interest:** No, I declare that the authors have no competing interests as defined by Nature Research, or other interests that might be perceived to influence the results and/or discussion reported in this paper.

#### References

- Sultana, J.; Islam, M.S.; Ahmed, K.; Dinovitser, A.; Ng, B.W.-H.; Abbott, D. Terahertz detection of alcohol using a photonic crystal fiber sensor. *Appl. Opt.* **2018**, *57*, 2426–2433. [[CrossRef](#)] [[PubMed](#)]
- Hamburg, M.A. *Advancing Regulatory Science*; American Association for the Advancement of Science: Washington, DC, USA, 2011; Volume 331, p. 987.
- Rachana, M.; Charles, I.; Swarnakar, S.; Krishna, S.V.; Kumar, S. Recent advances in photonic crystal fiber-based sensors for biomedical applications. *Opt. Fiber Technol.* **2022**, *74*, 103085. [[CrossRef](#)]

4. Triyana, K.; Sembiring, A.; Rianjanu, A.; Hidayat, S.N.; Riowirawan, R.; Julian, T.; Kusumaatmaja, A.; Santoso, I.; Roto, R. Chitosan-based quartz crystal microbalance for alcohol sensing. *Electronics* **2018**, *7*, 181. [[CrossRef](#)]
5. Pohanish, R.P. *Sittig's Handbook of Toxic and Hazardous Chemicals and Carcinogens*; William Andrew: Norwich, NY, USA, 2017.
6. Ayad, M.M.; Torad, N.L. Alcohol vapours sensor based on thin polyaniline salt film and quartz crystal microbalance. *Talanta* **2009**, *78*, 1280–1285. [[CrossRef](#)] [[PubMed](#)]
7. Iqbal, F.; Biswas, S.; Bulbul, A.A.-M.; Rahaman, H.; Hossain, M.B.; Rahaman, M.E.; Awal, M.A. Alcohol sensing and classification using PCF-based sensor. *Sens. Bio-Sens. Res.* **2020**, *30*, 100384. [[CrossRef](#)]
8. García-Cañas, V.; Simo, C.; Herrero, M.; Ibáñez, E.; Cifuentes, A. *Present and Future Challenges in Food Analysis: Foodomics*; ACS Publications: Washington, DC, USA, 2012.
9. Martinez, A.W.; Phillips, S.T.; Whitesides, G.M.; Carrilho, E. *Diagnostics for the Developing World: Microfluidic Paper-Based Analytical Devices*; ACS Publications: Washington, DC, USA, 2010.
10. Dzantiev, B.B.; Byzova, N.A.; Urusov, A.E.; Zherdev, A.V. Immunochromatographic methods in food analysis. *TrAC Trends Anal. Chem.* **2014**, *55*, 81–93. [[CrossRef](#)]
11. Wei, W.Y.; White, I.M. Inkjet-printed paper-based SERS dipsticks and swabs for trace chemical detection. *Analyst* **2013**, *138*, 1020–1025.
12. Ali, E.M.; Edwards, H.G. The detection of flunitrazepam in beverages using portable Raman spectroscopy. *Drug Test. Anal.* **2017**, *9*, 256–259. [[CrossRef](#)]
13. Ayad, M.M.; Salahuddin, N.; Minisy, I.M. Detection of some volatile organic compounds with chitosan-coated quartz crystal microbalance. *Des. Monomers Polym.* **2014**, *17*, 795–802. [[CrossRef](#)]
14. Pérez-Ponce, A.; Garrigues, S.; de La Guardia, M. Vapour generation–fourier transform infrared direct determination of ethanol in alcoholic beverages. *Analyst* **1996**, *121*, 923–928. [[CrossRef](#)]
15. Allan, J.T.; Geoffrey, H.L.; Easton, E.B. The effect of the gas diffusion layer on the performance of fuel cell catalyst layers in ethanol sensors. *Sens. Actuators B Chem.* **2018**, *254*, 120–132. [[CrossRef](#)]
16. Jung, Y.; Kim, J.; Awofeso, O.; Kim, H.; Regnier, F.; Bae, E. Smartphone-based colorimetric analysis for detection of saliva alcohol concentration. *Appl. Opt.* **2015**, *54*, 9183–9189. [[CrossRef](#)] [[PubMed](#)]
17. Hwang, R.-J.; Beltran, J.; Rogers, C.; Barlow, J.; Razatos, G. Measurement of uncertainty for blood alcohol concentration by headspace gas chromatography. *Can. Soc. Forensic Sci. J.* **2017**, *50*, 114–124. [[CrossRef](#)]
18. Ozoemena, K.I.; Musa, S.; Modise, R.; Ipadeola, A.K.; Gaolatlhe, L.; Peteni, S.; Kabongo, G. Fuel cell-based breath-alcohol sensors: Innovation-hungry old electrochemistry. *Curr. Opin. Electrochem.* **2018**, *10*, 82–87. [[CrossRef](#)]
19. Zhang, W.; Lang, X.; Liu, X.; Li, G.; Singh, R.; Zhang, B.; Kumar, S. Advances in tapered optical fiber sensor structures: From conventional to novel and emerging. *Biosensors* **2023**, *13*, 644. [[CrossRef](#)]
20. An, G.; Jia, P.; Liang, T.; Hong, Y.; Wang, H.; Ghaffar, A.; Xiong, J. Double-sided polished ultra-stable and ultra-sensitive optical fiber sensor. *Plasmonics* **2020**, *15*, 1471–1479. [[CrossRef](#)]
21. Hu, Y.; Hou, Y.; Ghaffar, A.; Liu, W. A narrow groove structure based plasmonic refractive index sensor. *IEEE Access* **2020**, *8*, 97289–97295. [[CrossRef](#)]
22. Cavinato, A.G.; Mayes, D.M.; Ge, Z.; Callis, J.B. Noninvasive method for monitoring ethanol in fermentation processes using fiber-optic near-infrared spectroscopy. *Anal. Chem.* **1990**, *62*, 1977–1982. [[CrossRef](#)]
23. Parthibavarman, M.; Sangeetha, S.; Renganathan, B.; BoopathiRaja, R. High-performance fiber optic gas sensor-based Co<sub>3</sub>O<sub>4</sub>/mwcnt composite by a novel microwave technique. *J. Iran. Chem. Soc.* **2019**, *16*, 2463–2472. [[CrossRef](#)]
24. Mitsushio, M.; Masunaga, T.; Yoshidome, T.; Higo, M. Alcohol selectivity and measurement of ethanol concentrations in liquors using teflon® af2400-coated gold-deposited surface plasmon resonance-based glass rod sensor. *Prog. Org. Coat.* **2016**, *91*, 33–38. [[CrossRef](#)]
25. Blum, P.; Mohr, G.J.; Matern, K.; Reichert, J.; Spichiger-Keller, U.E. Optical alcohol sensor using lipophilic Reichardt's dyes in polymer membranes. *Anal. Chim. Acta* **2001**, *432*, 269–275. [[CrossRef](#)]
26. Penza, M.; Cassano, G.; Aversa, P.; Antolini, F.; Cusano, A.; Cutolo, A.; Giordano, M.; Nicolais, L. Alcohol detection using carbon nanotubes acoustic and optical sensors. *Appl. Phys. Lett.* **2004**, *85*, 2379–2381. [[CrossRef](#)]
27. Chiam, Y.S.; Lim, K.S.; Harun, S.W.; Gan, S.N.; Phang, S.W. Conducting polymer coated optical microfiber sensor for alcohol detection. *Sens. Actuators A-Phys.* **2014**, *205*, 58–62. [[CrossRef](#)]
28. Morisawa, M.; Amemiya, Y.; Kohzu, H.; Liang, C.X.; Muto, S. Plastic optical fibre sensor for detecting vapour phase alcohol. *Meas. Sci. Technol.* **2001**, *12*, 877–881. [[CrossRef](#)]
29. Mitsushio, M.; Higashi, S.; Higo, M. Analyses of alcohols using a gold-deposited optical-fiber refractive index sensor system. *Bunseki Kagaku* **2003**, *52*, 433–438. [[CrossRef](#)]
30. Phang, S.W.; Yang, H.Z.; Harun, S.W.; Arof, H.; Ahmad, H. Simple fiber optic sensor based on tapered fiber for aliphatic alcohol detection. *J. Optoelectron. Adv. Mater.* **2011**, *13*, 604–608.
31. Hussain, S.; Ghaffar, A.; Musavi, S.H.A.; Mehdi, M.; Ahemd, M.; Jianping, Y.; Lei, C.; Mehdi, R.; Mehdi, I. Fiber optic sensor embedded in robotic systems for 3-D orientation assessment using polymer fiber. *Opt. Fiber Technol.* **2023**, *81*, 103559. [[CrossRef](#)]
32. Shi, J.; Ghaffar, A.; Li, Y.; Mehdi, I.; Mehdi, R.; Soomro, F.A.; Hussain, S.; Mehdi, M.; Li, Q.; Li, Z. Dynamic rotational sensor using polymer optical fiber for robot movement assessment based on intensity variation. *Polymers* **2022**, *14*, 5167. [[CrossRef](#)]

33. Ghaffar, A.; Li, Q.; Mehdi, M.; Hussain, S.; Jia, Y.M.; Onyekwena, C.C.; Xie, Q.; Ali, N. Analysis of Force Sensor Using Polymer Optical Fiber Based on Twisting Structure. *IEEE Sens. J.* **2022**, *22*, 23960–23967. [[CrossRef](#)]
34. Ghaffar, A.; Li, Q.; Mehdi, M.; Das, B.; Alvi, I.H.; Xie, Q.; Ma, J. Multiplexing sensors technique for angle and temperature measurement using polymer optical fiber. *Infrared Phys. Technol.* **2023**, *130*, 104585. [[CrossRef](#)]
35. Snyder, A.W. Coupled-mode theory for optical fibers. *JOSA* **1972**, *62*, 1267–1277. [[CrossRef](#)]
36. Snyder, A.W.; Love, J. *Optical Waveguide Theory*; Springer Science & Business Media: Berlin/Heidelberg, Germany, 2012.
37. Xia, F.; Song, H.; Zhao, Y.; Zhao, W.-M.; Wang, Q.; Wang, X.-Z.; Wang, B.-T.; Dai, Z.-X. Ultra-high sensitivity SPR fiber sensor based on multilayer nanoparticle and Au film coupling enhancement. *Measurement* **2020**, *164*, 108083. [[CrossRef](#)]
38. Ying, Y.; Si, G.-y.; Luan, F.-j.; Xu, K.; Qi, Y.-w.; Li, H.-n. Recent research progress of optical fiber sensors based on D-shaped structure. *Opt. Laser Technol.* **2017**, *90*, 149–157. [[CrossRef](#)]
39. Podder, E.; Jibon, R.H.; Hossain, M.B.; Bulbul, A.A.-M.; Biswas, S.; Kabir, M.A. Alcohol sensing through photonic crystal fiber at different temperature. *Opt. Photonics J.* **2018**, *8*, 309. [[CrossRef](#)]
40. Patrialova, S.N.; Hatta, A.M.; Sekartedjo, S. Alcohol sensor based on U-bent hetero-structured fiber optic. In Proceedings of the Second International Seminar on Photonics, Optics, and Its Applications (ISPhOA 2016), Bali, Indonesia, 24–25 August 2016; pp. 221–225.
41. Petrova, S.; Kostov, Y.; Jeffris, K.; Rao, G. Optical ratiometric sensor for alcohol measurements. *Anal. Lett.* **2007**, *40*, 715–727. [[CrossRef](#)]
42. Erfkamp, J.; Guenther, M.; Gerlach, G. Hydrogel-Based Sensors for Ethanol Detection in Alcoholic Beverages. *Sensors* **2019**, *19*, 1199. [[CrossRef](#)]

**Disclaimer/Publisher’s Note:** The statements, opinions and data contained in all publications are solely those of the individual author(s) and contributor(s) and not of MDPI and/or the editor(s). MDPI and/or the editor(s) disclaim responsibility for any injury to people or property resulting from any ideas, methods, instructions or products referred to in the content.